Catalysis Today 146 (2009) 241–247

Contents lists available at ScienceDirect

Catalysis Today

journal homepage: www.elsevier.com/locate/cattod

Improvement of the cyclic stability of high temperature CO_2 absorbent by the addition of oxygen vacancy possessing material

Kwang Bok Yi, Chang Hyun Ko, Jong-Ho Park, Jong-Nam Kim *

Chemical Process Research Center, Korea Institute of Energy Research, 71-2 Jang-dong, Yuseong-gu, Daejeon 305-343, Republic of Korea

ARTICLE INFO

Article history:
Available online 23 February 2009

Keywords:
CaO
Cyclic stability
Sorption enhanced hydrogen production
Oxygen mobility

ABSTRACT

Influences of oxygen vacancy possessing additives ($Ce_xZr_{1-x}O_2$, $LaAl_yMg_{1-y}O_3$) on the cyclic stability of Ca-based high temperature CO_2 absorbent were investigated. Compared to absorbents composed only of CaO, oxygen vacancy possessing materials added absorbents showed significantly improved cyclic stability in repeated CO_2 absorption/desorption. It has been also found that the cyclic stability of CO_2 absorbent was proportional to the availability of oxygen vacancy in additives. It was presumed that oxygen vacant site behaves as a jump site for facilitating CO_2 diffusion through the product layer formed during carbonation.

1. Introduction

Carbonation of calcium oxide has been studied for the various industrial applications such as CO_2 capture from power plant flue gas [1], coal gasification [2], sorption enhanced hydrogen production [3–10], and energy storage [11,12]. Among the technologies, the specific interest of this study lies on the sorption enhanced hydrogen production (SEHP).

SEHP seems particularly attractive because it produces highly concentrated hydrogen with simultaneous capturing of CO_2 that is ready for compression and transportation. SEHP has several additional advantages over the conventional multi-step hydrogen production which includes endothermic steam methane reforming and water–gas shifting followed by hydrogen purification [7]. SEHP accomplishes reforming, shift, and purification in a single processing step. These reactions occur simultaneously in the presence of a reforming catalyst and high temperature CO_2 absorbent. The simultaneous and overall reactions can be represented as follows:

Reforming:

$$CH_4(g) + H_2O(g) \leftrightarrow CO(g) + 3H_2(g)$$

Shift:

$$CO(g) + H_2O(g) \leftrightarrow CO_2(g) + H_2(g)$$

CO_2 removal:

$$CaO(s) + CO_2(g) \leftrightarrow CaCO_3(s)$$

Overall:

$$CH_4(g) + 2H_2O(g) + CaO(s) \leftrightarrow CaCO_3(g) + 4H_2(g)$$

Conventional steam methane reforming reaction occurs at around 850 °C and 25 bar. SEHP can be carried out at lower temperature and pressure. Lopez and Harrison [6] performed SEHP using calcined dolomite at about 650 °C and 15 bar achieving almost complete conversion of CH_4. Yi and Harrison [7] showed that SEHP can be carried out even at 440 °C and atmospheric pressure obtaining over 90 vol% of hydrogen and extremely low CO concentration (<40 ppmv, dry basis) in product. As proven in the literature [3], no shift catalyst is required in SEHP. Additional benefit from using SEHP is that the combined reactions are almost thermally neutral so that no supplemental energy is required for hydrogen production [6,7]. Thermodynamic study [13] has shown that auto-thermal steam bio-oil reforming while utilizing CaO as CO_2 absorbent is feasible. However, the SEHP requires supplemental energy to regenerate the used CO_2 absorbent for multi-cycle operation. Nevertheless, the supplemental energy for SEHP is expected to be about 20% less than the one required in conventional reforming process [6]. Even with the above advantages, there are fundamental obstacles for the successful commercialization of SEHP. The most obvious drawback is the CO_2 capacity deteriorating tendency of the absorbent over multi-cycle operation [14]. It has been reported that CO_2 capacity of the absorbent dropped to 20% of the initial capacity after 10–20 cycles of SEHP [6,15,16]. The reasons for CO_2 capacity deterioration are known as pore blockage and absorbent

* Corresponding author. Tel.: +82 42 860 3112; fax: +82 42 860 3102.
E-mail addresses: cosy32@kier.re.kr (K.B. Yi), chko@kier.re.kr (C.H. Ko), jhpark@kier.re.kr (J.-H. Park), jnkim@kier.re.kr (J.-N. Kim).

0920-5861/$ – see front matter © 2009 Elsevier B.V. All rights reserved.
doi:10.1016/j.cattod.2008.12.009

sintering [14]. The CO_2–CaO reaction proceeds through two reaction steps. The first step is the rapid surface reaction and the second step is the slow diffusion of CO_2 through $CaCO_3$ layer formed during early stage of carbonation [1]. As the cycle number increases the CaO particles are agglomerated with sintering providing less surface area. Barker [17] claimed that the critical thickness, the thickness of $CaCO_3$ layer that is formed before diffusion takes over the rate controlling, over CaO particle is 22 nm. The sintering or pore blockage caused by multi-cycle absorption/desorption drives the absorption reaction to the direction of slow diffusion control. Until recently, CO_2 capacity decay of CaO was considered to be inevitable when it goes through multi-cycle absorption/desorption at elevated temperature. If other components that are inert for the reaction with CO_2 are present in the absorbent CaO agglomeration can be decelerated. Bandi [18] investigated CaO containing natural minerals and claimed that increased concentration of inert part in absorbent would positively affect the cyclic stability. It is true that inert part takes a role in maintaining micro-structure of the absorbent because the inert part behaves as skeleton during the reaction preventing severe agglomeration of the active material. However, the addition of inert part slows down the agglomeration but absorbent particle will eventually agglomerate after long time exposure at elevated temperature. Considering the fact that commercial reforming catalyst is replaced every two or three years, the successful development of SEHP requires absorbent stability guaranteed for more than two years. Recently, Li et al. [10,19,20] successfully produced CO_2 absorbent possessing excellent cyclic stability and performed multi-cycle SEHP with the developed absorbent. They claim that incorporation of $Ca_{12}Al_{14}O_{33}$ into CaO improved the cyclic stability by forming skeleton preventing agglomeration. However, the explanation does not seem complete.

Among the few reports about the reaction mechanism of CaO with CO_2, Bhatia and Perlmutter [21] suggested the ion migration of CO_3^{2-} and O^{2-} ions to explain diffusion through the product layer. Our group was inspired by this suggestion and made an assumption that ion migration facilitating additives would enhance the cyclic stability of absorbent. Therefore, in this study, mono-, bi-, and tri-metal oxides that possess oxygen vacancy have been chosen as additives to facilitate ion migration and the cyclic stabilities of absorbent containing the additives were compared with that of absorbent composed only of CaO. The CaO based absorbents with or without additives were prepared by identical preparation method and their cyclic stability in isothermal CO_2 absorption/desorption were compared. In addition, new absorption/desorption mechanism is proposed when CaO based absorbents with additives that possess oxygen vacancy are used.

2. Experiments

2.1. Samples preparation

Absorbents used in this study are CaO, CaO/ZrO_2, CaO/$Ce_xZr_{1-x}O_2$ (x = 0.25, 0.5, 0.8), CaO/$LaAlO_3$, and CaO/$LaAl_{0.8}Mg_{0.2}O_3$. All the additives are well-known materials for possessing oxygen vacancies. All raw chemicals were reagent-grade and purchased from Aldrich. Each sample was prepared by exactly the same method for clear comparison. For example, the preparation method for pure CaO is as follows. First, CaO (calcium oxide, 25 g) was weighted and added into distilled water (700 mL). This mixture was heated to 75 °C on a heating plate and stirred for 2 h. Then white cloud-like suspension occurred as the hydration of CaO proceeded. This hydration process involves volume expansion resulting in cracking of particles. The resultant mixture was dried in a ventilating oven until dried powder was obtained. The powder was retrieved after complete drying and then moved to a furnace and heated at 500 °C for 3 h. The heat-treated powder was slowly cooled to room temperature and crushed. Then the crushed mixture was heated to 900 °C and annealed for another 3 h. After being cooled, the powder was crushed and sieved for test. For additive incorporation, precursors of additives were added after the hydration process. After additional stirring for 2 h at 75 °C, the rest of the procedure was followed in the same manner mentioned above. This method allowed obtaining uniform dispersion of additives across the entire absorbent particle. Precursors for the additives were: $ZrO(NO_3)_2{\cdot}6H_2O$ for ZrO_2 addition, $Ce(NO_3)_3{\cdot}6H_2O$ and $ZrO(NO_3)_2{\cdot}6H_2O$ $6H_2O$ for $Ce_xZr_{1-x}O_2$ (x = 0.25, 0.5, 0.8), $La(NO_3)_3{\cdot}4H_2O$ and $Al(NO_3)_3{\cdot}9H_2O$ for $LaAlO_3$ addition, $Mg(NO_3)_2{\cdot}6H_2O$, $La(NO_3)_3{\cdot}4H_2O$, $4H_2O$, and $Al(NO_3)_3{\cdot}9H_2O$ for $LaAl_{0.8}Mg_{0.2}O_3$ addition. Precursor amount to be added was carefully calculated to result in 25 wt% of the fixed additive content for all absorbents.

Fornasiero et al. [22] performed temperature-programmed reduction (TPR) in a H_2/Ar (10/90) mixture of Rh-loaded CeO_2–ZrO_2 solid solutions with the ZrO_2 content varying between 10 and 90 mol% and found that 20 mol% of ZrO_2 provided maximum reduction tendency. They found that incorporation of ZrO_2 into a solid solution with CeO_2 strongly promotes bulk reduction of the solid solution in comparison to that of pure CeO_2. Trovarelli et al. [23] performed TPR using CeO_2–ZrO_2 solid solutions and the degree of reduction and H_2 consumed was a maximum when the ZrO_2 content was 20 mol%. Hori et al. [24] reported an increase in oxygen mobility by a factor of 1.7–2.5 for phase-separated CeO_2–ZrO_2 compared to CeO_2 alone and by 3–5 for solid solutions of CeO_2–ZrO_2 and the optimum zirconia concentration was 25 mol%. Similar results have been presented by Luo et al. [25].

Therefore, when ceria zirconia is added in this study, the atomic ratio of Ce to Zr was carefully varied to directly compare cyclic stabilities of absorbents along with oxygen mobility variation. Molecular composition and names of samples are shown in Table 1.

2.2. Absorbent characterization

X-ray diffraction pattern of absorbents was recorded on an X-ray diffractometer (XRD, Rigaku D/Max2000-Ultima Plus, Cu-Kα radiation, λ = 0.15418 nm, 30 kV, 20 mA) in the range of 2θ = 10–70°. Typical peaks of CaO are expected to be present in XRD patterns of all samples. Additives were identified by indexing the peaks on the XRD patterns. Also, morphologies of the prepared absorbents were observed by a scanning electron microscope (SEM, Philips XL30, 15 kV). The surface areas of absorbents were measured by nitrogen adsorption–desorption at −196 °C on a Micrometics ASAP 2010 analyzer. The resolution was 0.133 Pa for the system. Each absorbent was degassed at 150 °C and <1.33 mPa for 16 h before measurement.

2.3. Experimental procedure

Prepared sample was crushed and sieved to have a particle size of 100–150 μm. Then around 40–60 mg of sample was placed in a thermogravimetric analyzer (TGA, TA instrument Q50) for

Table 1
Sample names and compositions of CaO based absorbents.

Sample name	Molecular formula	Weight ratio of CaO to additive
Ca100	CaO	1
Ca75Zr	CaO/ZrO_2	3
Ca75CeZr1/3	CaO/$Ce_{0.25}Zr_{0.75}O_2$	3
Ca75CeZr1	CaO/$Ce_{0.5}Zr_{0.5}O_2$	3
Ca75CeZr4	CaO/$Ce_{0.8}Zr_{0.2}O_2$	3
Ca75LaAl	CaO/$LaAlO_3$	3
Ca75LaAlMg4	CaO/$LaAl_{0.8}Mg_{0.2}O_3$	3

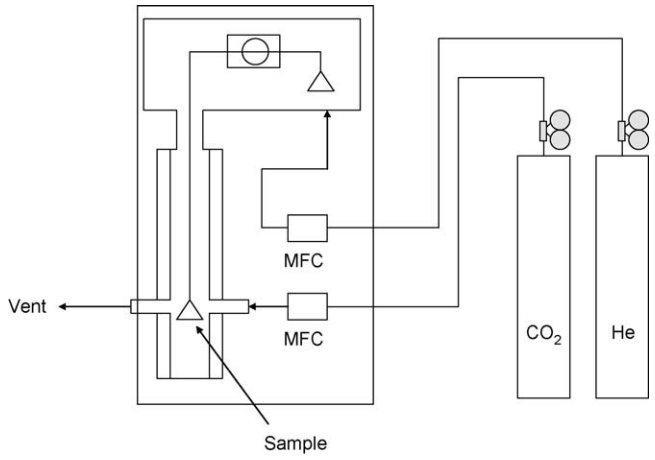

Scheme 1. Experimental setup.

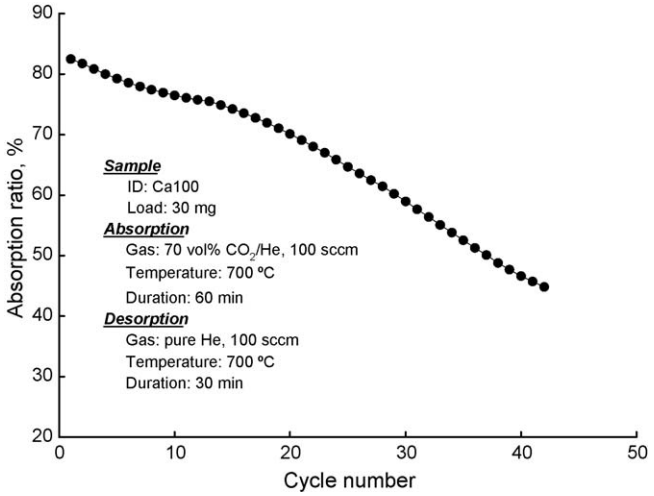

Fig. 1. Absorption ratio changes of pure CaO (Ca100) over multi-cycle absorption/desorption test in TGA.

Table 2
Operating condition for TGA.

	Absorption		Desorption	
Temperature	700 °C			
Gas	He	30 sccm	He	30 sccm
	CO_2	70 sccm	CO_2	0 sccm
Duration	60 min		30 min	
Sample load	40–60 mg			
Sample particle diameter	100–150 μm			

absorption/desorption cyclic tests. The schematic diagram of experimental setup is shown in Scheme 1. He and CO_2 cylinders were connected to the TGA and the flow rate was controlled by mass flow controllers (MFCs) installed inside the TGA. In order to protect the balance chamber of TGA, He flowed through the chamber at all time. When absorption test was in action, CO_2 flowed to sample chamber. Then the CO_2 was replaced by He with the flow rate fixed when the system is switched to desorption mode. Detailed operating conditions are shown in Table 2. Once the sample chamber was heated to 700 °C for initial absorption, the temperature was maintained until the test was terminated.

Desorption rate of CO_2 is dependant on CO_2 partial pressure and temperature. Generally, desorption of CO_2 caused by carbonate decomposition occurs much faster at higher temperature. Therefore, usual desorption temperature in many studies is in the range of 800–950 °C. The reason for choosing isothermal condition for absorption/desorption in this study was for eliminating effects of frequent temperature changes on cyclic stability.

3. Results and discussion

For comparison purpose, CO_2 absorption capacities of absorbents prepared in this study were represented by absorption ratio, a CaO-basis normalized value. The absorption ratio is mole percentage of CaO converted to $CaCO_3$:

$$\text{Absorption ratio } (\%) = \frac{\text{moles of } CO_2 \text{ absorbed in sorbent}}{\text{moles of CaO in sorbent}} \times 100$$

As a reference material, the pure CaO (Ca100) was prepared, characterized and tested. Fig. 1 shows absorption ratio changes of Ca100 over multi-cycle absorption/desorption test in TGA. Due to the hydration process applied for the preparation of Ca100, the initial absorption ratio of Ca100 was over 80% which is presumed to be very high. However, as reported elsewhere, the absorption ratio of Ca100 rapidly decreased as cycle number increased. When it passed 40th cycle, its absorption ratio was only 40%, which is half of the initial value. Absorption and desorption rates of Ca100 were also recorded over multi-cycle test and are shown in Fig. 2. As described in the previous section, absorption is clearly divided into

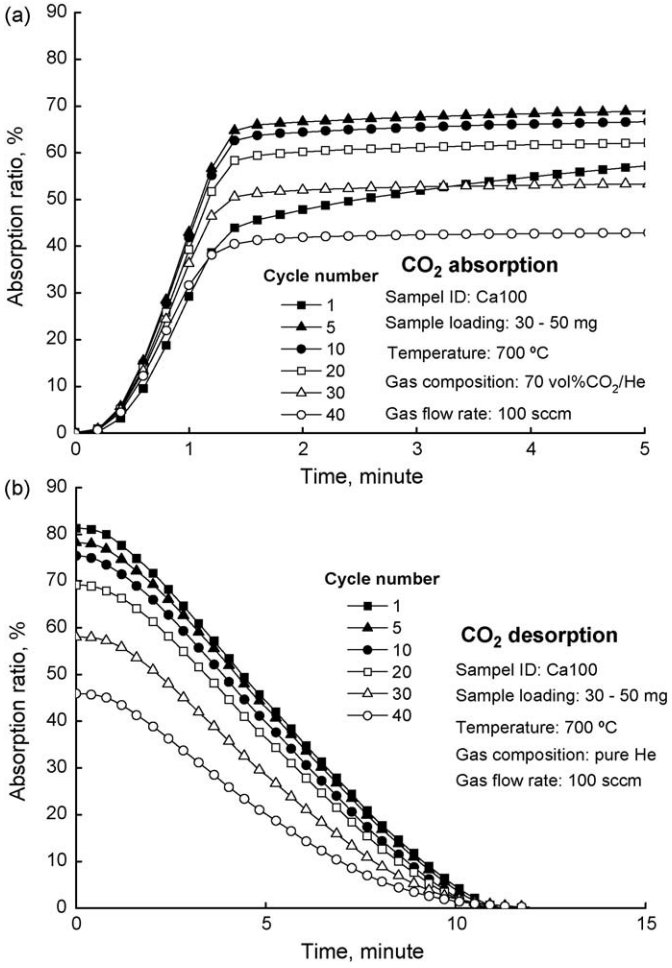

Fig. 2. Absorption (a) and desorption (b) rate changes of pure CaO (Ca100) over multi-cycle test in TGA.

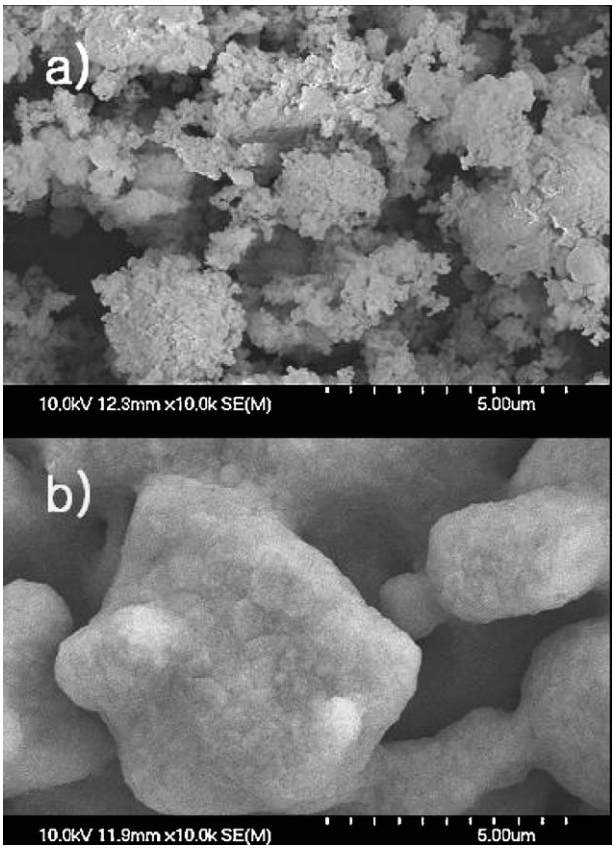

Fig. 3. Scanning electron microscope images of Ca100: (a) fresh as synthesized and (b) after 40 cycles.

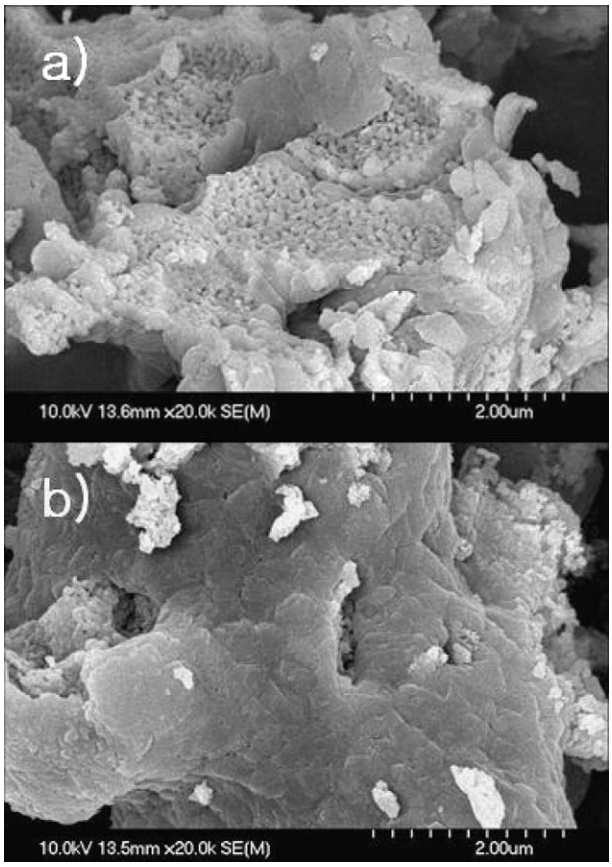

Fig. 4. Scanning electron microscope images of Ca75CeZr4: (a) fresh as synthesized and (b) after 40 cycles.

two regimes: kinetic controlled regime where the absorbent take up CO_2 rapidly at the early stage of absorption and diffusion controlled regime that CO_2 take-up rate is very slow. As the cycle number increased, the portion of absorbent under kinetic control became smaller resulting in the decrease of absorption ratio while the transition point where diffusion control taking over kinetic control remained the same at around 1.5 min. Desorption rates over multi-cycle also decreased as the cycle number increased as shown in Fig. 2b. This degradation of CO_2 capacity has been attributed to the blockage of pore and sintering caused by high temperature and repetitive absorption/desorption. The SEM images shown in Fig. 3 provid more visual explanation. The fresh Ca100 has average particle size of about 50 nm and repeated absorption and desorption of CO_2 to 40 cycles caused severe agglomeration with the growth of particles size to 5 μm.

3.1. Cerium zirconate addition

Fluorite type CeO_2 and ZrO_2 are well-known oxygen vacancy possessing materials. It has been proven in the literature that solid solution of CeO_2–ZrO_2 creates more oxygen vacancies than CeO_2 alone. According to Hori et al. [24], degrees of the oxygen vacancy of solid solutions in the ZrO_2 concentration range of 15–50 mol% is very high and do not vary significantly while more than 50 mol% ZrO_2 provides significant decrease in oxygen vacancy. With this background, CaO based absorbents containing 25 wt% of $Ce_xZr_{1-x}O_2$(x = 0.25, 0.5, 0.8); Ca75CeZr1/3, Ca75CeZr, and Ca75CeZr4 were prepared in our laboratory and their cyclic stabilities in TGA tests were compared. Among the prepared absorbents, morphology of Ca75CeZr4 sample was analyzed using SEM. As shown in Fig. 4a, fresh Ca75CeZr4 sample possesses well-developed microscopic structure. After 40 cycles of absorption and desorption, however, great degree of agglomeration occurred as shown in Fig. 4b. Nevertheless, there exist initial shape maintained particles unlike the case of Ca100. It is assumed that pore blockage and sintering were prevented with certain degree by the additive. The TGA test results of $CaO/Ce_xZr_{1-x}O_2$ are shown in Fig. 5 along with Ca100. TGA test results of additive containing absorbents are quite different from that of Ca100. While the absorption ratio of Ca100 continuously decreased from the very first cycle as cycle

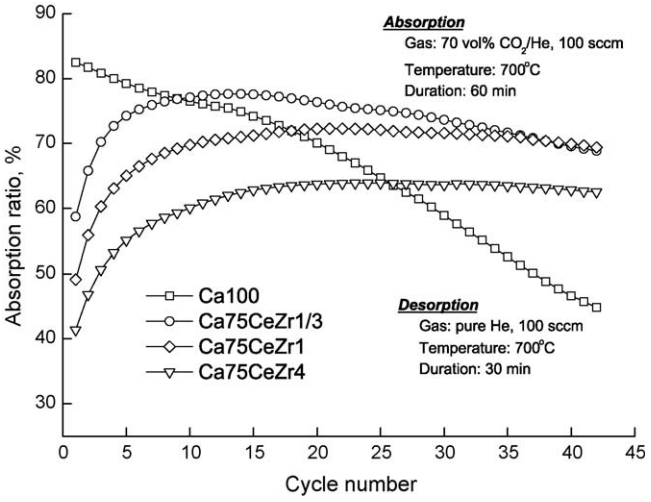

Fig. 5. Absorption ratio changes of $CaO/Ce_xZr_{1-x}O_2$ and pure CaO over multi-cycle absorption/desorption test in TGA.

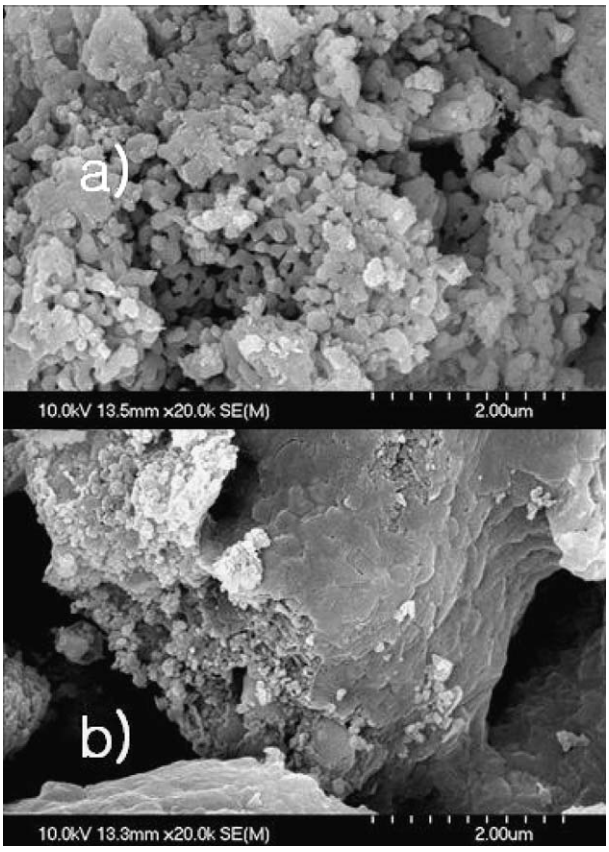

Fig. 6. Scanning electron microscope images of Ca75Zr: (a) fresh as synthesized and (b) after 40 cycles.

number increased, all of the additive containing absorbents showed rapid absorption ratio increase in the early stage of multi-cycle absorption/desorption tests and maintained their CO_2 absorption capacities to some extent. For example, the absorption ratio of Ca75CeZr4 showed 42% at the end of first absorption, gradually increased to 64% at around 25 cycles, and stabilized with slight decrease. This result implies that oxygen vacancy helps the absorbents to achieve better cyclic stability than Ca100. Even more reinforcing evidence is that enhanced cyclic stability is directly proportional to degree of oxygen mobility that additives have. For example, stability degradation tendency of absorption ratios after 25 cycles has following order: Ca100 > Ca75CeZr1/3 > Ca75CeZr > Ca75CeZr4. Based on this result, it is suggested that an oxygen vacancy available site in the additives behaves as an oxygen donor to provide O^{2-} ion to CO_2 forming CO_3^{2-} and this CO_3^{2-} is converted to CO_2 giving O^{2-} back to the site while receiving O^{2-} from the next site. By this manner, CO_2 can move around freely in additives until it meets CaO forming $CaCO_3$. That is, the additives not only prevent sintering and pore blockage but also provide the oxygen ion branches which take the role of lubricant to help CO_2 to slide into the core of absorbent.

3.2. Zirconia-only addition

In order to investigate the effect of less oxygen vacancy possessing material on the cyclic stability of CO_2 absorbent, CaO/ZrO_2 (Ca75Zr) absorbent was prepared with the identical method used above. According to the literature [26–28], the activation energy for oxygen diffusion in ZrO_2 is more than twice of that in CeO_2–ZrO_2 solid solution. SEM images of Ca75Zr sample are shown in Fig. 6. The SEM images of fresh Ca75Zr and after 40 cycles of

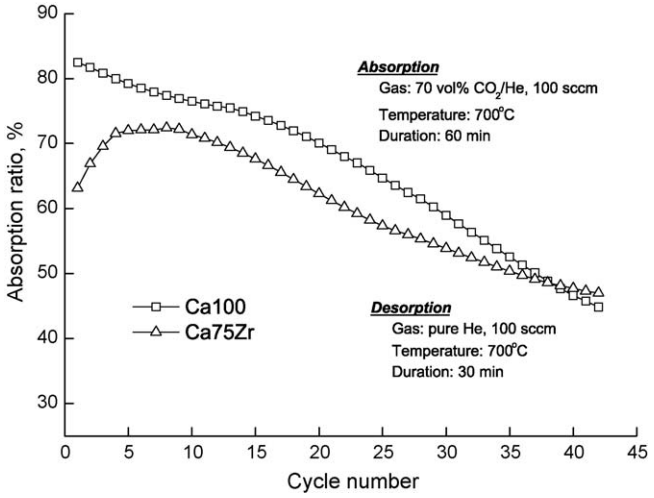

Fig. 7. Absorption ratio changes of CaO/ZrO2 and pure CaO over multi-cycle absorption/desorption test in TGA.

absorption/desorption are similar to those of Ca75CeZr4. Agglomeration and sintering after 40 cycles are much less severe than those of Ca100. However, TGA test result shown in Fig. 7 implies that the cyclic stability of Ca75Zr is not improved at all. Ca75Zr showed the maximum absorption ratio, 72% at about 6th cycle. Thereafter the ratio continuously decreased as the cycle number increased by similar degradation degree of Ca100. In order to clarify this tendency of cyclic stability degradation, XRD analysis has been performed. XRD patterns of Ca100, Ca75Zr, and Ca75CeZr4 are shown in Fig. 8. As expected, peaks of Ca100 clearly indicate that the sample consists of only CaO and these peaks identically appeared in Ca75Zr and Ca75CeZr4. Meanwhile, ZrO_2 was not found in Ca75Zr. Instead, additional peaks appeared and they were identified as $CaZrO_3$. Thermodynamic analysis using commercial software (HSC chemistry, Outokumpu) has shown that $CaZrO_3$ is readily formed rather than remaining as separate phases when CaO and ZrO_2 are exposed to elevated temperature. Dudek and Bućko [29] found out $CaZrO_3$ possesses very high oxygen vacancy only when 2 mol% of CaO is present in excess. When the content of CaO is more than that of $CaZrO_3$, the mixture completely loses its oxygen storage capacity. Therefore, it is presumed than Ca75Zr does not have any oxygen vacancy. On the other hand, additional peaks in Ca75CeZr4 were identified as CeO_2 and any

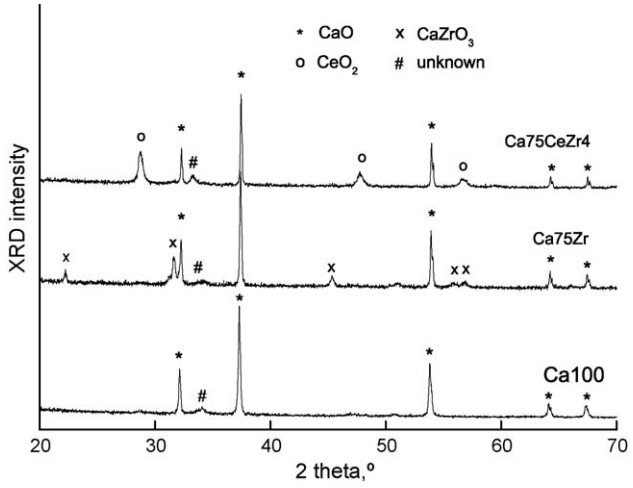

Fig. 8. The XRD diffraction patterns of Ca100, Ca75Zr, and Ca75CeZr4.

Table 3
BET specific surface areas of CO_2 absorbents.

Sample name	Molecular formula	Specific surface area (m^2/g)
Ca100	CaO	42.12
Ca75Zr	CaO/ZrO_2	4.54
Ca75CeZr1/3	$CaO/Ce_{0.25}Zr_{0.75}O_2$	5.44
Ca75CeZr1	$CaO/Ce_{0.5}Zr_{0.5}O_2$	4.34
Ca75CeZr4	$CaO/Ce_{0.8}Zr_{0.2}O_2$	2.71
Ca75LaAl	$CaO/LaAlO_3$	4.49
Ca75LaAlMg4	$CaO/LaAl_{0.8}Mg_{0.2}O_3$	4.36

other peaks did not appear. When the CeO_2 with ZrO_2 forms $Ce_xZr_{1-x}O_2$ as a solid solution there will be only slight shift of the CeO_2 peaks in the XRD pattern instead of showing ZrO_2 peaks as separate phase. It is assumed that assigned peaks as CeO_2 are actually indicating the presence of $Ce_xZr_{1-x}O_2$ in Ca75CeZr4. Therefore, oxygen vacancies are available in $Ce_xZr_{1-x}O_2$ containing samples such as Ca75CeZr1/3, Ca75CeZr1, and Ca75CeZr4. This is additional evidence that oxygen vacancy of the additive might help to improve the cyclic stability of CO_2 absorbent.

3.3. BET surface area measurement

Specific surface areas of all samples were measured before being tested in TGA. The measured values are shown in Table 3. If the additives behave more as structure supporter that prevent sintering than as oxygen ion donor that facilitate CO_2 diffusion the assumption made in this study may not be valid. However, obtained specific surface area values of fresh samples eliminate the possibility that the effect of preventing sintering is dominant on improvement of the cyclic stability. The specific surface areas of all the samples were in the range of 2–6 m^2/g except Ca100. It is very difficult for micro-pores to exist in this range and the results leave little possibility that surface reaction is dominant at the early stage of multi-cycle test in TGA. In Ca100 case, the BET surface area measurement result fits well with the conventional theory that sintering is the main cause of CO_2 capacity deterioration as shown in the SEM analysis.

3.4. Lanthanum based additives

In order to check if the assumption that oxygen vacancy possessing additives improves cyclic stability of CO_2 absorbent can be applied to other than cerium based materials, lanthanum aluminate ($LaAlO_3$) and Mg added lanthanum aluminate ($LaAl_{0.8}Mg_{0.2}O_3$) were selected as additives. XRD patterns of Ca75LaAl and Ca75LaAlMg4 are shown in Fig. 9. Intensities of

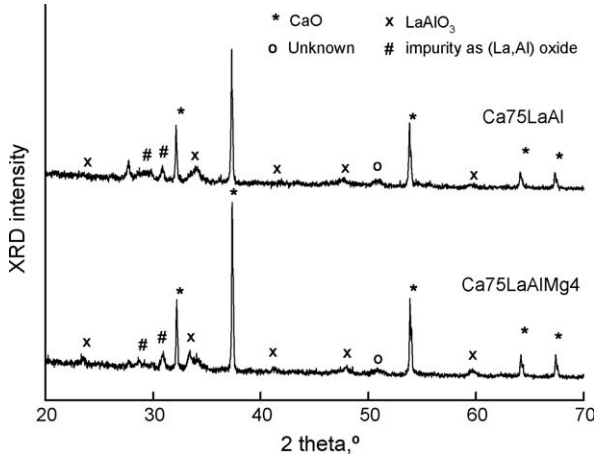

Fig. 9. The XRD diffraction patterns of Ca75LaAl and Ca75LaAlMg4.

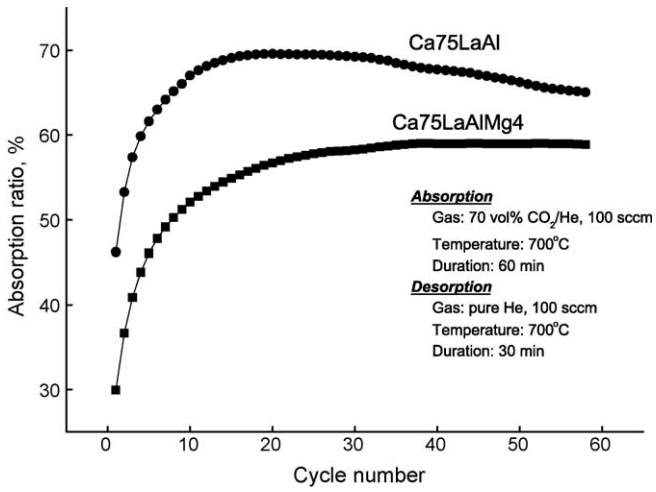

Fig. 10. Absorption ratio changes of Ca75LaAl and Ca75LaAlMg4 over multi-cycle absorption/desorption test in TGA.

$LaAlO_3$ peaks appeared to be very weak yet big enough to be assigned. Two patterns shown in Fig. 9 are almost identical. Since no separate phase except impurities appeared in the patterns, successful formation of solid solution was assumed. Nguyen et al. [30] measured ion conductivity of $LaAlO_3$ and B-site partially substituted $LaAlO_3$ with Mg and found out that partial substitution of Al with Mg increased oxygen vacancy and ion conductivity. Therefore, the better cyclic stability was expected for Ca75AlMg4. The same TGA test procedure used for Ca100 and others above was applied to Ca75LaAl and Ca75LaAlMg4. The result of multi-cycle test is shown in Fig. 10. CO_2 absorption capacity of Ca75LaAl over multi-cycle tends to degrade yet not severe as Ca100. However, Ca75LaAlMg4 sample showed no sign of CO_2 absorption capacity degradation. This result is consistent with those obtained from cerium zirconate containing absorbents above.

3.5. Absorption rates of CO_2 absorbent in multi-cycle test

In order to check if oxygen vacancy possessing materials affect absorption rate in diffusion controlled region, absorption rates of all samples were measured during the multi-cycle test in TGA. In Fig. 11, absorption rates at 40th cycle are shown. CO_2 absorption rate of Ca75LaAl in surface reaction controlled region was faster than any other absorbent. The rest of them showed similar rates. In

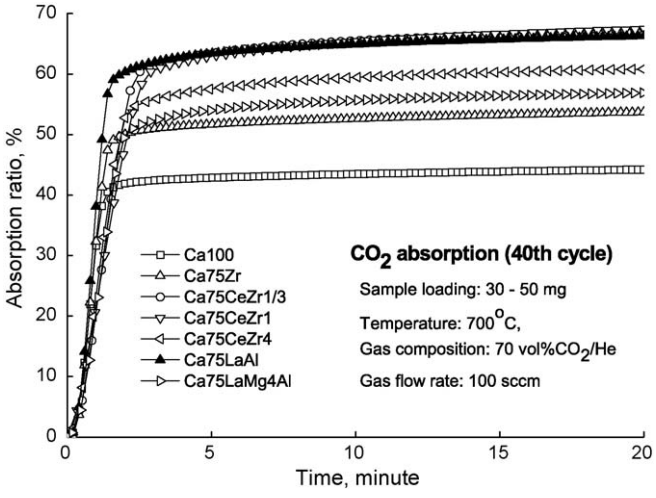

Fig. 11. Absorption rates of CO_2 absorbent at 40th cycle in TGA test.

diffusion controlled region, Ca75Zr and Ca100 showed identically the slowest rate. Compared to these two rates, absorbent with oxygen vacancy possessing additives showed faster absorption rate. Especially, the absorption rates in transition region from surface reaction to diffusion controlled region showed differences more clearly. While Ca100 and Ca75Zr showed sharp transition to diffusion controlled region, other absorbents containing oxygen vacancy showed smooth transition. That is, oxygen vacancy possessing additives help for the absorbents to keep absorbing CO_2 with faster rate even in diffusion controlled region.

4. Conclusions

The motivative assumption of this study was that the additives possessing oxygen vacancy sticks out oxygen ion branches and CO_2 infused into CO_2 absorbent can easily form CO_3^{2-} and leave the oxygen ion, then move to next oxygen ion branch as maintaining form of CO_3^{2-}. By this manner, CO_2 can easily reach CaO available inside of the agglomerated or even sintered CO_2 absorbent.

It was found that the addition of oxygen vacancy possessing materials into high temperature CO_2 absorbent (CaO) improved cyclic stability. Cerium zirconate added CaO actually showed improved cyclic stability as Ce/Zr ratio increased. Among the tested absorbents, Ca75CeZr4 ($CaO/Ce_{0.8}Zr_{0.2}O_2$, weight ratio: 3/1) showed the best cyclic stability. The addition of lanthanum aluminate with B-site partially substituted by Mg also showed better cyclic stability than lanthanum aluminate addition, which also indicates that if additives possess higher oxygen vacancies better cyclic stability can be achieved. Attempt for ZrO_2 addition into CaO actually resulted in $CaZrO_3$ formation. Since $CaZrO_3$ mixed with excess CaO possesses no oxygen vacancy, $CaO/CaZrO_3$ absorbent (Sample ID: Ca75Zr) did not show any improvement in cyclic stability. Moreover, the small specific surface area values and SEM analysis data supported the assumption that oxygen vacancy possessing materials facilitate CO_2 diffusion.

References

[1] H. Gupta, L.S. Fan, Ind. Eng. Chem. Res. 41 (2002) 4035.
[2] S.Y. Lin, Y. Suzuki, H. Hatano, M. Harada, Energy Fuels 15 (2001) 339.
[3] C. Han, D.P. Harrison, Chem. Eng. Sci. 49 (1994) 5875.
[4] S.F. Wu, H.T. Beum, J.I. Yang, J.N. Kim, Ind. Eng. Chem. Res. 46 (2007) 7896.
[5] S.F. Wu, Q.H. Li, J.N. Kim, K.B. Yi, Ind. Eng. Chem. Res. 47 (2008) 180.
[6] O.A. Lopez, D.P. Harrison, Ind. Eng. Chem. Res. 40 (2001) 5102.
[7] K.B. Yi, D.P. Harrison, Ind. Eng. Chem. Res. 44 (2005) 1665.
[8] N. Hilenbrand, J. Readman, I.M. Dahl, R. Blom, Appl. Catal. A 303 (2006) 131.
[9] J.C. Abanades, E.S. Rubin, E.J. Anthony, Ind. Eng. Chem. Res. 43 (2004) 3462.
[10] Z.S. Li, N.S. Cai, Y.Y. Huang, H.J. Han, Energy Fuels 19 (2005) 1447.
[11] Y. Kato, D. Saku, N. Harada, Y. Yoshizawa, Prog. Nucl. Energy 32 (1998) 563.
[12] K. Kyaw, T. Shibata, F. Watanabe, H. Matsuda, M. Hasatani, Energy Convers. Manage. 38 (1997) 1025.
[13] A.A. Iordanidis, P.N. Kechagiopoulos, S.S. Voutetakis, A.A. Lemonidou, I.A. Vasalos, Int. J. Hydrogen Energy 31 (2006) 1058.
[14] A.I. Lysikov, A.N. Salanov, A.G. Okunev, Ind. Eng. Chem. Res. 46 (2007) 4633.
[15] J.C. Abandes, Chem. Eng. J. 90 (2002) 303.
[16] M. Silaban, P. Narcida, D.P. Harrison, Chem. Eng. Commun. 146 (1996) 149.
[17] R.J. Barker, Appl. Chem. Biotechnol. 23 (1973) 733.
[18] A. Bandi, in: Proceedings of the 5th International Symposium on Gas Cleaning at High Temperature, 17–20 September, Session 7, Paper No. 7, 2002.
[19] Z.S. Li, N.S. Cai, J.B. Yang, Ind. Eng. Chem. Res. 45 (2006) 8788.
[20] Z.S. Li, N.S. Cai, Y.Y. Huang, Ind. Eng. Chem. Res. 45 (2006) 1911.
[21] S.K. Bhatia, D.D. Perlmutter, AIChE J. 29 (1983) 79.
[22] P. Fornasiero, R.D. Monte, G.R. Rao, J. Kaspar, S. Meriani, A. Trovarelli, M. Graziani, J. Catal. 151 (1995) 168.
[23] A. Trovarelli, F. Zamar, J. Llorca, C. De Leitenburg, G. Dolcetti, J.T. Kiss, J. Catal. 169 (1997) 490.
[24] C.E. Hori, A. Brenner, K.Y. Simon Ng, K.M. Rahmoeller, D. Belton, Catal. Today 50 (1999) 299.
[25] M.F. Luo, G.L. Lie, X.M. Zheng, J. Mater. Sci. Lett. 17 (1998) 1553.
[26] A.A. Safonov, A.A. Bagatur'yants, A.A. Korkin, Micro. Eng. 69 (2003) 692.
[27] U. Brossmann, R. Wurschum, U. Sodervall, H.E. Schaefer, J. Appl. Phys. 85 (1999) 7646.
[28] J.H. Lee, S.M. Yoon, B.K. Kim, J. Kim, H.W. Lee, H.S. Song, Solid State Ionics 144 (2001) 175.
[29] M. Dudek, M.M. Bućko, Solid State Ionics 157 (2003) 183.
[30] T.L. Nguyen, M. Dokiya, S. Wang, H. Tagawa, T. Hashimoto, Solid State Ionics 130 (2000) 229.